Scanning Microscopy

Volume 6 | Number 2 Article 13

4-8-1992

Scanning Electron Microscopy and Energy-Dispersive X-Ray Microanalysis Studies of Early Dental Calculus on Resin Plates Exposed to Human Oral Cavities

T. Kodaka
Showa University

Y. Ohohara
Ohohara Dental Clinic

K. Debari
Showa University

Scanning Microscopy, Vol. 6, No. 2, 1992 (Pages 475-486)
Scanning Microscopy International, Chicago (AMF O'Hare), IL 60666 USA

0891-7035/92$5.00+.00

SCANNING ELECTRON MICROSCOPY AND ENERGY-DISPERSIVE X-RAY MICROANALYSIS STUDIES OF EARLY DENTAL CALCULUS ON RESIN PLATES EXPOSED TO HUMAN ORAL CAVITIES

T. Kodaka*, Y. Ohohara[1] and K. Debari[2]

Second and [2]First Departments of Oral Anatomy, School of Dentistry,
Showa University, Tokyo 142, Japan
[1]Ohohara Dental Clinic, Sekiyado-cho, Higashi-Katsishika-gun, Chiba 270-02, Japan

(Received for publication January 18, 1992, and in revised form April 8, 1992)

Abstract

Dental calculus formed after 10 days on resin plates, applied to the lingual sides of the mandibular gingival regions in eight human subjects, was investigated by means of scanning electron microscopy (SEM) and energy-dispersive X-ray microanalysis (EDX). The mineral deposits were mainly divided into three types: A, B, and C. The type A deposits showing an average Ca/P molar ratio of 1.42 were densely packed with fine needle-shaped crystals formed by the intra- and extracellular calcification. The type A deposits, probably composed of Ca-deficient apatites and the transitional forms between apatite and octacalcium phosphate (OCP), were observed in all subjects. The type B deposits showing an average Ca/P molar ratio of 0.96 were aggregated with polygonal column, triangular plate-shaped, and rhombohedral crystals. These crystals identified as brushite ($CaHPO_4$-$2H_2O$: dicalcium phosphate dihydrate: DCPD) were found in four subjects. Platelet-shaped crystals of the type C deposits were observed in three subjects. Their Ca/P molar ratio of 1.26 and the crystal shape were similar to those of OCP. Whitlockite crystals were not found although Mg-containing hexagonal disk-like crystals were observed in two subjects.

Key Words: Resin plate, oral cavity, early dental calculus, scanning electron microscopy, energy-dispersive X-ray microanalysis, crystal shape, Ca/P molar ratio, brushite (DCPD).

*Address for Correspondence:
Tetsuo Kodaka
Second Department of Oral Anatomy
School of Dentistry, Showa University
1-5-8 Hatanodai, Shinagawa-ku
Tokyo 142, Japan

Telephone No.: (81)-3-3784 8157
FAX No.: (81)-3-3786 0072

Introduction

Among the major inorganic constituents of human dental calculus, brushite [$CaHPO_4$-$2H_2O$: dicalcium phosphate dihydrate: DCPD], octacalcium phosphate [$Ca_8(PO_4)_4(HPO_4)_2 5H_2O$: OCP], hydroxyapatite [$Ca_{10}(PO_4)_6(OH)_2$: HAP], and β-tricalcium phosphate or whitlockite [$Ca_{10}(HPO_4)(PO_4)_6$: WHT] have been revealed in X-ray diffraction analyses [17, 20, 21, 52, 60]. Their native and synthetic crystal habits are as follows; DCPD is a triangular plate, polygonal column, and rhombohedral in shape [3, 4, 34, 37, 40-42, 46, 51]; OCP is needle-, ribbon-, flake-, and plate-like in shape [6, 8, 36-39, 42, 46, 49]; HAP is hexagonal dipyramidal and needle- or rod-like in shape [6, 25, 37, 46, 49, 54]; while WHT is rhombohedral and cuboidal in shape [11, 15, 42, 49, 54].

Crystal identification in human dental calculus has been mainly performed by transmission electron microscopy (TEM) with electron diffractions [16, 27, 53, 55, 58, 63]. Based on this method, the long ribbon-shaped crystals were determined to be OCP [55], the fine needle-shaped crystals to be HAP [16, 53, 58], and the rhombohedral crystals to be WHT [27, 63], whereas the fine hexagonal column-shaped crystals in early calculus, 4 to 8 days old [57] and young calculus, 3 months old [58], were suggested to be DCPD by Schroeder [58, 59]. Using scanning electron microscopy (SEM), needles or elongated shapes, different shapes and sizes of platelet forms, and cuboidal crystals were observed in old dental calculus [43].

The ideal molar calcium to phosphorous ratios (Ca/P) for different calculus phosphates are as follows: 1.00 for DCPD [3, 4, 12, 37, 52]; 1.33 for OCP [6, 12, 37, 49, 52]; 1.67 for HAP [6, 12, 25, 37, 49, 52]; and 1.29 to 1.43 for magnesium (Mg) containing WHT [$Ca_9Mg(HPO_4)(PO_4)_6$] [7, 12, 26]. Such Ca/P molar ratios and crystal shapes can be used as the indicators of biological calcium phosphate crystals.

From crystal shapes and Ca/P molar ratios based on examination with a SEM and a SEM fitted with an EDX system [28-32], we classified three kinds of calcium phosphate crystals in old dental calculus as follows; fine grain-shaped HAP [29, 32], variably plate-

Table 1. Subjects, sex, age, and number of crystals masses analyzed by SEM-EDX

Subject (No.)	Sex	Age (years)	Analyzed mass (No.)
I	Male	42*	#1 - #6
II	Female	25	#1 - #5
III	Female	22	#1 - #5
IV	Male	36*	#1 - #4
V	Male	37*	#1
VI	Male	22*	#1 - #3
VII	Male	24	#1 - #3
VIII	Male	33	#1 - #3

*smoker

shaped OCP [29, 31, 32], and hexahedrally based Mg-containing WHT [28-30]. In these studies, DCPD crystals were not observed. Kani *et al.* [24] using microbeam X-ray diffraction analysis, also did not find DCPD, although Grøn *et al.* [17] reported that DCPD occurred infrequently and only in small amounts.

Schroeder and Bambauer [60] reported that DCPD was most frequent in young supragingival calculus deposits ranging in age from 22 to 27 days and less in old ones, whereas HAP and WHT were detectable more frequently in old than in young calculus deposits, and that OCP occurred in addition to DCPD in the earliest stages of development of dental calculus and was also one of the main constituents in old calculus. Morphologically Schroeder and his co-workers [57-59, 61] proposed that during the formation of dental calculus, two mineralization centers of type A and B should be distinguished and suggested that the crystals of A- and B-centers were formed by HAP and DCPD, respectively.

In the present study, using resin plates exposed to human oral cavities for 10 days, we illustrate the three-dimensional shape of calcium phosphate crystals which have not been investigated in the early stages of dental calculus formation by means of SEM and SEM-EDX, although there were a number of studies on early calculus up to 14 days of age [16, 44, 45, 47, 56, 57, 61] and young calculus ranging in age from 22 days to 3 months [44, 58, 60] using weight measurement [45], chemical analysis [55], light microscopy [44, 47, 56, 61, 64], TEM [57, 61], TEM with electron diffractions [16, 58], and X-ray diffraction analysis [60]. In addition, these crystals and their frequency were compared with that of early, young, and old dental calculus reported previously.

Materials and Methods

For this experiment, an acrylic dental resin plate fitted with simple clasps was applied to the lingual side of mandibular incisors of the gingival region in eight human subjects aged 22 to 42 years (Table 1), who had no systematic nor salivary gland diseases. The subjects (I-VIII) were allowed to remove the resin plates during meals and tooth brushing. An exposure period of the resin plate to the oral environment of 10 days, similar to that used in previous studies [16, 45, 47, 56, 57, 61], was selected.

The resin plates with attached dental plaque and calculus deposits were fixed in 70% ethanol for one day, and the regions with the deposits were cut into small pieces of an area of about 1 x 1 cm^2 with a diamond wheel under running tap water. Several large masses of the deposits were removed from the resin plates with tweezers. About half of the specimens were rinsed in distilled water, dried in the air, and coated with carbon in a Hitachi HUS-5GB high vacuum evaporator; so that the principal elements of dental plaque and the mass which involved much the same crystals in shape and size could be analyzed at 5 points in quantity and quality by using a Hitachi X-560 SEM fitted with a Kevex 7000Q EDX (SEM-EDX). The number of the analyzed crystal masses in each subject (I-VIII) were up to 6 (#1-#6 in Table 1). The microprobe conditions were 15 kV accelerating voltage and $1x10^{-7}$ mA specimen irradiation current. The standard sample for quantitative analysis of Ca and P was native fluorapatite. Sulphur (S) and Mg were not quantitatively analyzed. The remaining specimens were treated with about 10% sodium hypochlorite (NaOCl) for one hour, in order to remove organic matter [22, 23, 29, 30, 32]. They were rinsed in running tap and distilled water, and dried in the air. All specimens treated with and without NaOCl were coated with a 10 to 15 nm thick platinum-palladium layer in an Eiko IB-5 ion sputtering apparatus and photographed by a Hitachi S-430 SEM operating at 20 kV.

Results

Macroscopically, the deposits on the resin plates, white in color, showed no distinction between dental calculus and plaque. These deposits were attached to the cervical edges of the resin plates, with their outer surfaces exposed to the oral cavity, and their inner surface adjacent to the gingiva, although their areas and volumes varied.

Figures 1 to 6 show the scanning electron micrographs of early dental calculus including type A deposits (without and with NaOCl in Figs. 1 and 2); type B deposits (without and with NaOCl in Figs. 3 and 4); and new type C deposits and others (Figs. 5 and 6).

Under the SEM-EDX analysis followed by the SEM observation, dental plaque containing microorganisms and no crystals occasionally showed a smooth surface (Figs. 1a-c). From such a plaque, S, Ca, and P were detected qualitatively, although the S content was rather small, and the Ca and P concentrations by weight were 2.30 $\pm$ 2.73 and 2.29 $\pm$ 2.01% (Mean $\pm$ S.D., n = 25; 5 samples x 5 points). In other deposits except for the plaque, the tightly packed masses, in various shapes and sizes, showing bacterial molds and microorganisms on the surfaces (type A: Figs. 1a-d, 3e), and

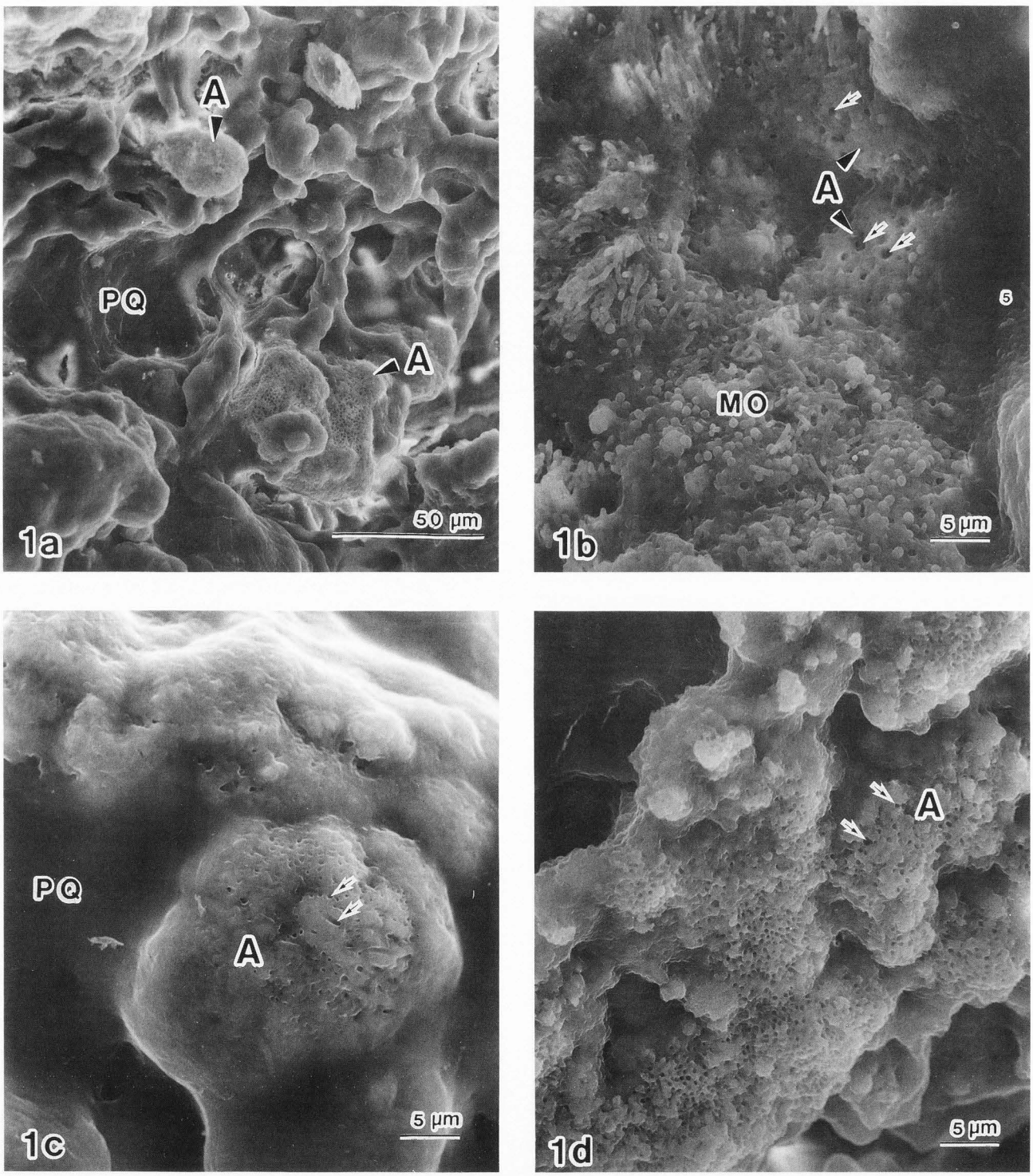

Figs. 1a-d. SEM micrographs of the natural surfaces of the type A deposits. Samples were not treated with NaOCl. Bacterial molds (arrows) on the tightly packed masses (A: type A deposits), microorganisms (MO, particularly in **b**), and plaque (PQ) showing a smooth surface are seen.

Table 2. SEM-EDX analysis of the type A deposits as shown in Figures 1a-d and 3e.

Sample (No.)	Ca (weight%)	P (weight%)	Ca/P (molar)
I-#1	21.49	12.68	1.31
II-#1	31.23	17.06	1.42
#2	28.79	16.03	1.39
#3	26.65	14.55	1.42
III-#1	30.97	17.33	1.39
#2	30.45	17.43	1.35
#3	28.57	15.31	1.44
#4	21.69	11.35	1.49
IV-#1	30.05	16.93	1.38
#2	28.79	15.63	1.43
V-#1	25.82	15.22	1.32
VI-#1	26.63	12.41	1.73
VII-#1	27.75	15.99	1.35
#2	26.84	14.11	1.48
VIII-#1	27.41	15.01	1.41
#2	26.48	15.13	1.34
Mean of 5 points; I - VIII: subjects; #1 - #4: a number of analyzed masses			
Total	27.48 ±2.84	15.14 ±1.79	1.42 ±0.10

Mean ± S.D. (n = 80: 16 samples x 5 points)

Table 3. SEM-EDX analysis of the type B deposits as shown in Figures 3a-e.

Sample (No.)	Ca (weight%)	P (weight%)	Ca/P (molar)
I-#2	22.25	17.26	1.00
#3	21.73	17.66	0.95
#4	21.60	17.65	0.95
#5	20.54	16.15	0.98
II-#4	23.40	19.01	0.95
#5	23.29	18.67	0.97
VI-#2	19.06	15.85	0.93
#3	18.45	15.36	0.90
VIII-#3	18.99	14.73	1.00
Mean of 5 points; I, II, VI, VII: subjects; #2 - #5: a number of analyzed masses			
Total	21.03 ±1.87	16.93 ±1.48	0.96 ±0.03

Mean ± S.D. (n = 45: 9 samples x 5 points).

Table 4. SEM-EDX analysis of the type C deposits as shown in Figures 5a,b.

Sample (No.)	Ca (weight%)	P (weight%)	Ca/P (molar)
I-#6	25.10	15.67	1.24
III-#5	24.95	15.02	1.29
VII-#3	11.89	7.51	1.24
Mean of 5 points; I, III, VII: subjects; #3, 5, 6: a number of analyzed masses			
Total	20.65 ±7.58	12.73 ±4.54	1.26 ±0.03

Mean ± S.D. (n = 15: 3 samples x 5 points)

---

aggregations of visualized crystals under the lower SEM observation with no treatment (type B: Figs. 3a-e; type C: Figs. 5a,b) were distinguishable. From these masses and aggregations, larger amounts of Ca and P were detected (Tables 2-4); therefore, the type A, B, and C deposits were recognized as calcium phosphate calculus.

The type A deposits shown in Figures 2a, 2b, 3e, and 6b formed by intra- and/or extracellular calcification were found in all subjects I to VIII. Fine needle-shaped crystals were observed on the surfaces (Fig. 2b). Table 2 shows the mineral content of the type A deposits. The Ca and P concentrations were 27.48 ± 2.84 and 15.14 ± 1.79%, respectively (Mean ± S.D., n =80; 16 samples x 5 points). The Ca/P molar ratio was 1.42 ± 0.10 ranging from 1.31 to 1.73, but most of the deposits showed an average less than 1.49 except for one subject (sample VI-#1 in Table 2).

The type B deposits shown in Figures 3a-e and 4a-e clearly differed from the type A deposits. The large crystals, frequently deposited on and between the masses of the type A deposits, mainly showed polygonal columnar and triangular plate-like shapes, but rarely a rhombohedral shape. Their sizes measured about 2 to 20 μm in length. Table 3 shows the mineral content of type B deposits observed in four resin plates (subjects I, II, VI, VIII). The Ca and P concentrations were 21.03 ± 1.87 and 16.93 ± 1.48%, respectively (Mean ± S.D., n = 45; 9 samples x 5 points). The Ca/P molar ratio was 0.96 ± 0.03 ranging from 0.90 to 1.00. The Ca concentration and the Ca/P molar ratio of the type B deposits were significantly lower ($p < 0.01$) than those of the type A deposits, although there was no significant difference ($p < 0.05$) in the P concentration (Tables 2, 3).

Masses of flake or platelet-like crystals were observed on rare occasion in limited areas of three resin plates (Figs. 5a, 5b; subject I, III, VII). The Ca and P concentrations were 18.40 ± 7.65 and 11.35 ± 4.62%, respectively (Mean ± S.D., n = 15; 3 samples x 5 points). The Ca/P molar ratio was 1.25 ± 0.03 ranging

Table 5. Variation of the crystal composition in eight subjects.

	Type			
Subject	A	B	C	Others
I	+1	+2	+1	/
II	+3	+2	/	+1**
III	+3	/	+1	+1*,**
IV	+3	/	/	+1*,**
V	+2	/	/	/
VI	+1	+2	/	/
VII	+3	/	+1	/
VIII	+3	+1	/	/

+3: large amounts and frequently
+2: small amounts but frequently
+1: small amounts and rarely
/: not found
*:oval-shaped crystals
**: hexagonal disk-like crystals

from 1.24 to 1.29 (Table 4). These crystals were categorized into the type C deposits. Statistically, the Ca/P molar ratio was significantly lower ($p < 0.01$) than that of the type A deposits, and higher ($p < 0.01$) than that of the type B deposits (Tables 2 to 4).

In two subjects, oval-shaped crystals measuring about 1 to 3 μm in length were rarely seen (Fig. 6a; subject III, IV). The Ca and P concentrations were 25.84 $\pm$ 2.19 and 14.29 $\pm$ 1.14%, respectively (sample IV-#4; Mean $\pm$ S.D. n = 5), and the Ca/P molar ratio was 1.40 $\pm$ 0.05. Calcium phosphate crystals containing a small amount of Mg were found in some areas of three resin plates attached with the type A and B deposits (Figs. 4e, 6b; subject II, III, IV). The crystals measuring about 3 μm in maximum length showed hexagonal disk-like shape, but the Ca, P, and Mg concentrations could not be quantitatively analyzed by the SEM-EDX due to the very small masses of the crystals.

The variation of the crystal composition of early dental calculus formed after 10 days in eight subjects is summarized in Table 5. When the frequency of type A is compared with that of type B deposits, four subjects showed type A only, one subject had a larger volume of type A than type B, one subject clearly showed type A and B, and two subjects had a relatively larger volume of type B than type A.

Discussion

Schroeder [56] reported that there were no differences between early (up to 12 days old) and old supragingival calculus in their percentage Ca and P contents of the deposit's ash. The Ca content in 12 days old calculus (31%) was similar to that of the type A deposits (27.5% in Table 2) rather than that of the type B deposits (21.0%), while the P content (19%) was similar to

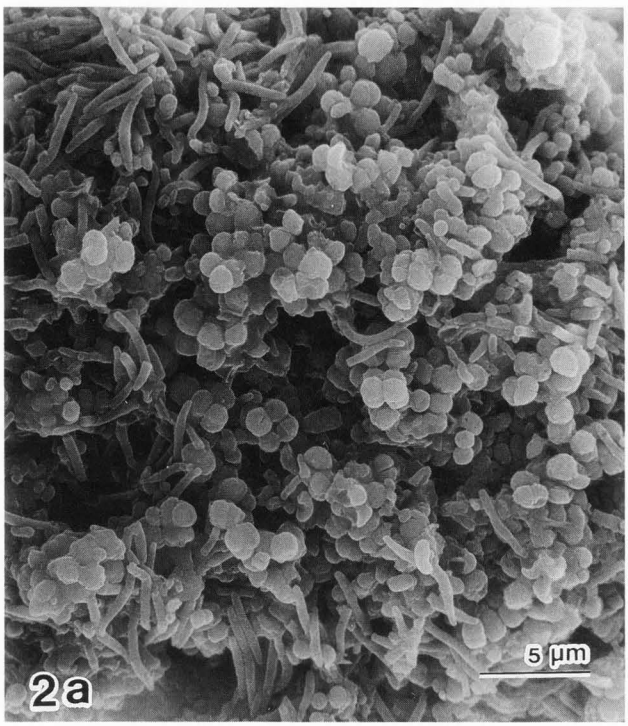

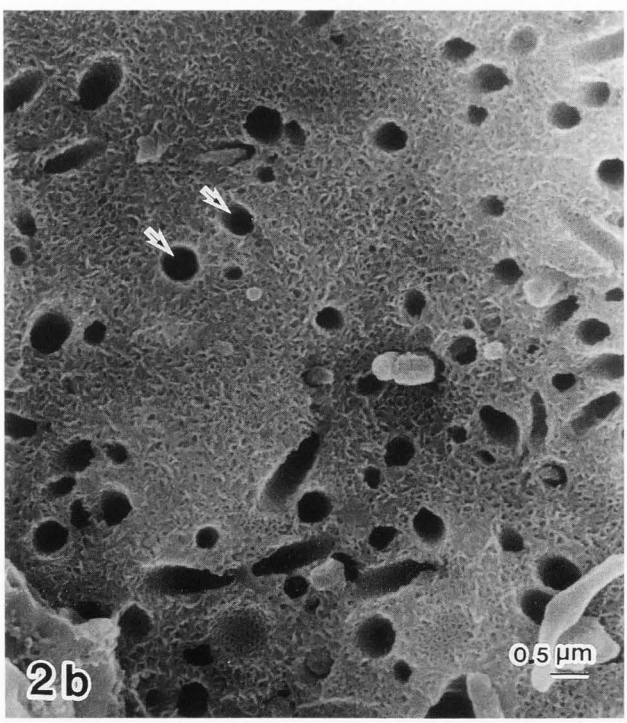

Figs. 2a,b. SEM micrographs of the A type deposits. Samples were treated with NaOCl. **a**: Intracellular calcification of bacteria on the fractured surface. **b**: Extracellular calcification showing fine needle-shaped crystals and bacterial molds (arrow).

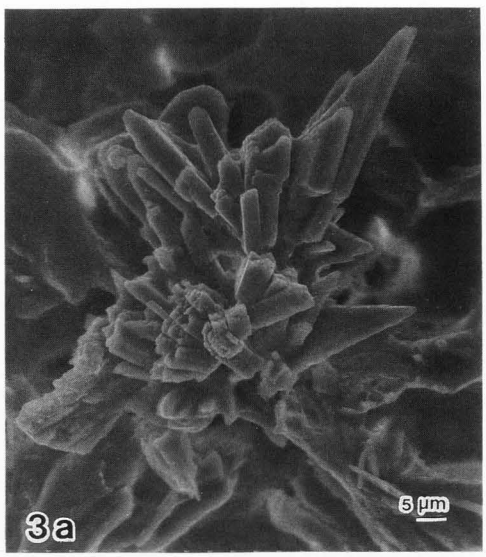

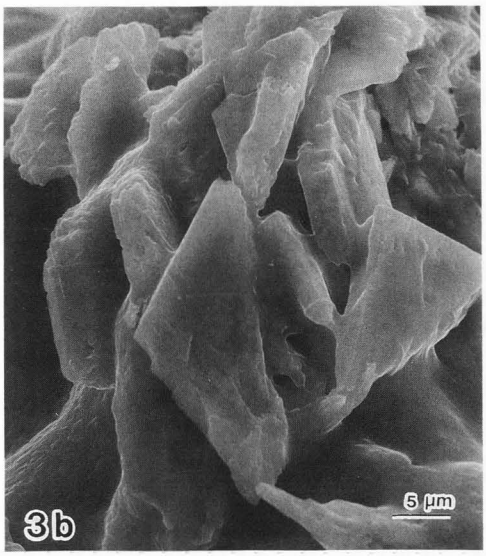

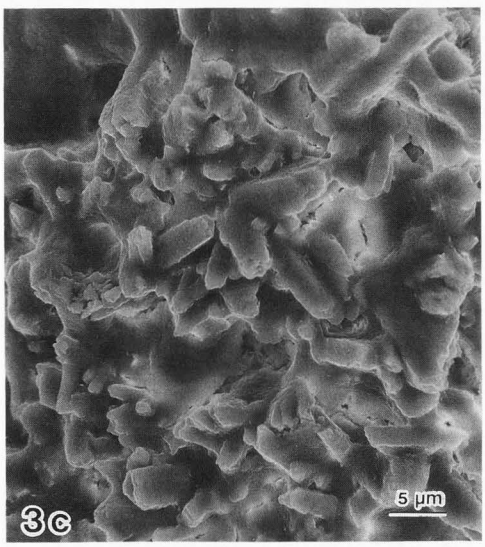

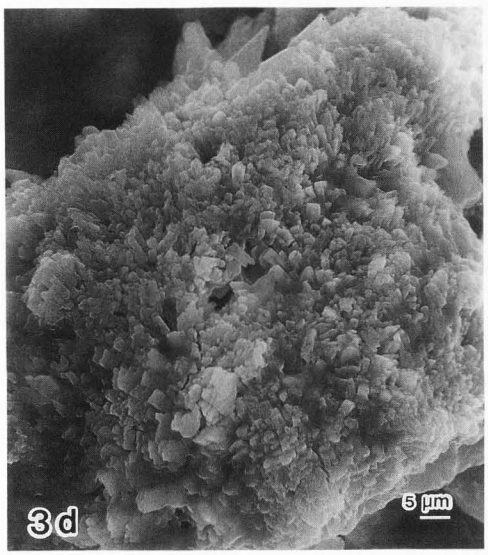

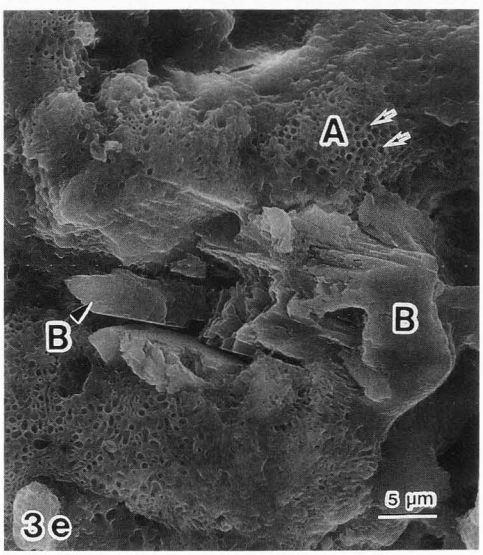

Figs. 3a-e. SEM micrographs of the natural surfaces of the B type deposits. Samples were not treated with NaOCl. Various sized crystals show polygonal columnar (**a, c-e**) and triangular plate-like shapes (**a, b**). In **e**, the B type deposits (B) exist between the type A deposits (A). Arrows: bacterial molds.

---

that of the type B deposits (16.9% in Table 3) rather than that of the type A deposits (15.1%). Schroeder [57-59] and his co-workers [61] proposed that during the formation of dental calculus, two mineralization centers of type A and B should be distinguished, and suggested that the crystals of A-centers formed by intra- and extracellular calcification was hydroxyapatite (HAP) while crystals of B-centers were brushite (DCPD).

In the present study, we classified the crystals of early dental calculus formed after 10 days into three types A, B, C, and the others, except for dental plaque.

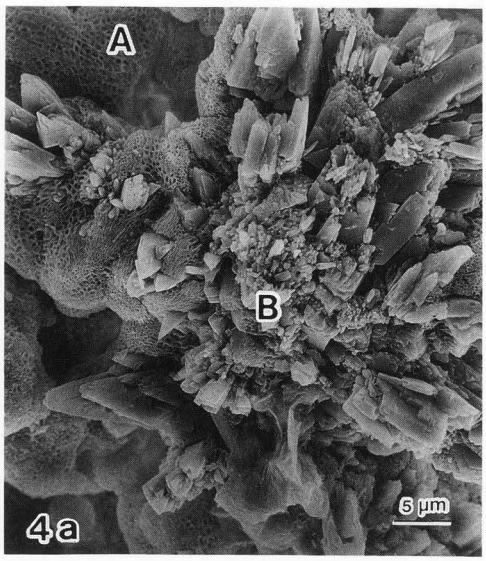

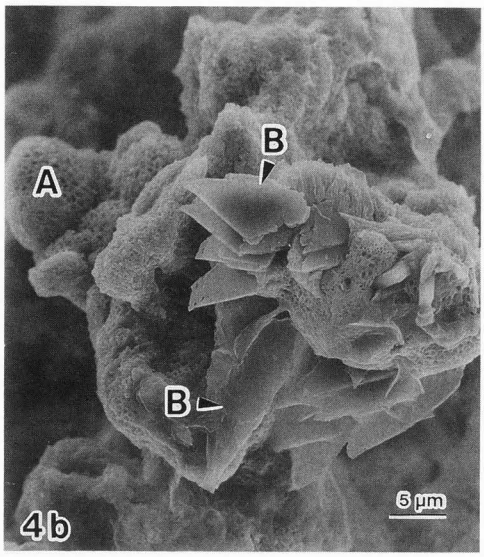

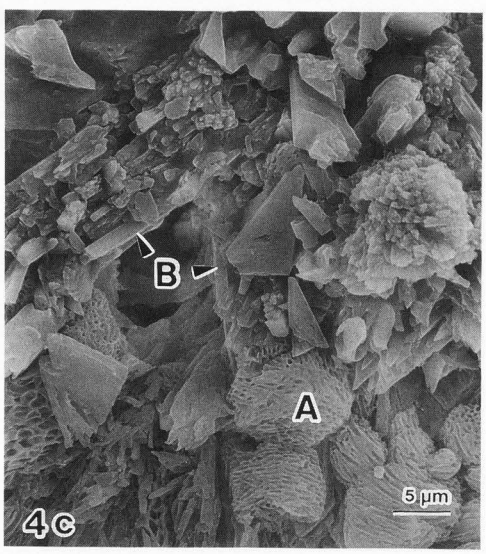

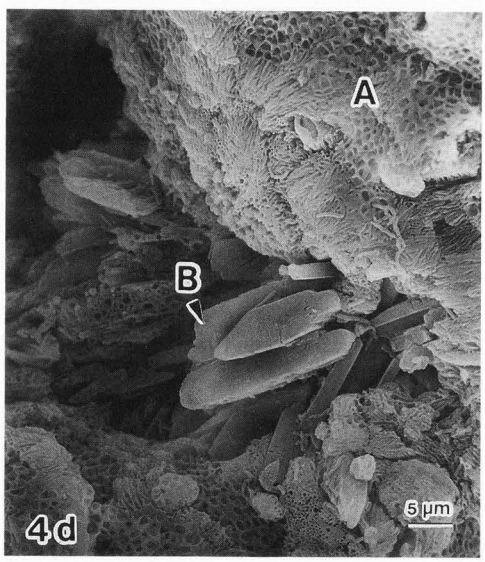

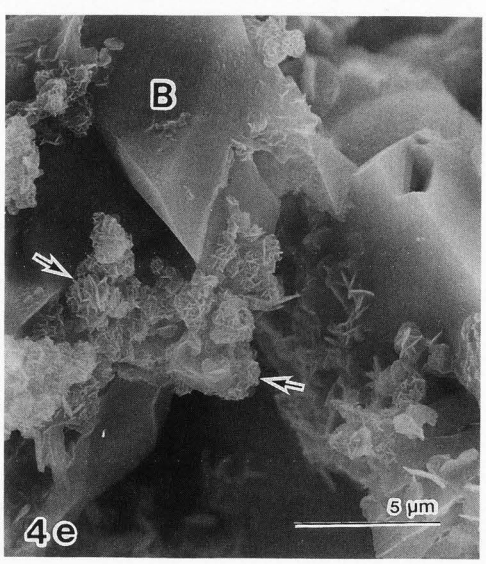

Figs. 4a-e. SEM micrographs of the type B deposits. Samples were treated with NaOCl. Various sized crystals show polygonal columnar (**a-d**) and triangular plate-like shapes (**a-c**), and rarely show a rhombohedral shape (**e**). These B type deposits (B) frequently exist on and between the A type deposits (A). An arrow in e shows hexagonal disk-like crystals (also see Fig. **6b**).

Fine needle-shaped crystals of the type A deposits resembled HAP rather than octacalcium phosphate (OCP) on account of the crystal shapes and the Ca/P molar ratios (Fig. 2b; Table 2) [6, 12, 25, 29, 32, 37, 46, 49, 52-54, 57-59]. Most of the crystal masses showed less than 1.67 of HAP in the Ca/P molar ratio; they may be Ca-deficient HAP [37, 50] or defective HAP [5, 12], but some of them might be transitional forms between OCP and HAP (OCP-HAP) [2, 6, 37-39, 48, 49]. Only in one case of the type A deposits, the Ca/P molar ratio

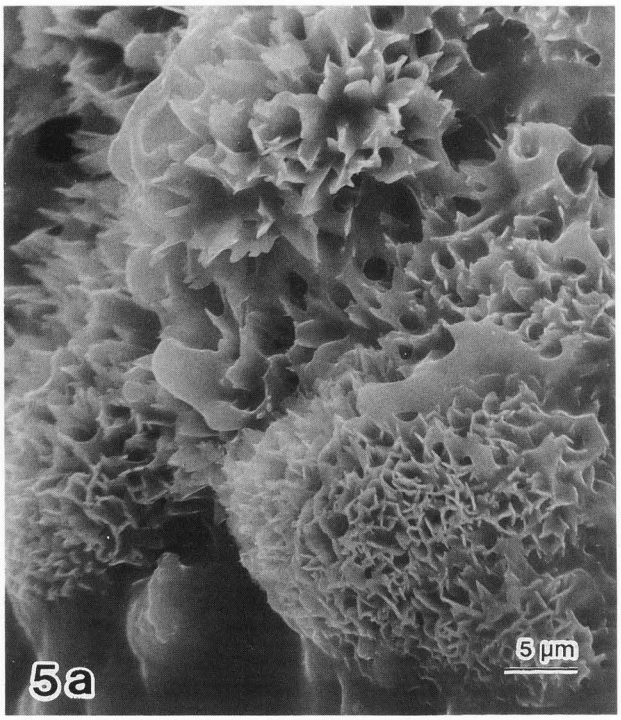

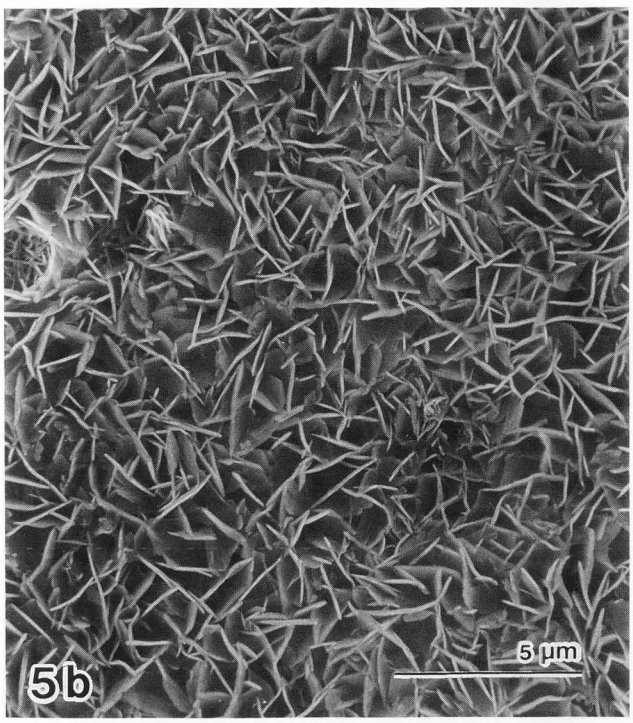

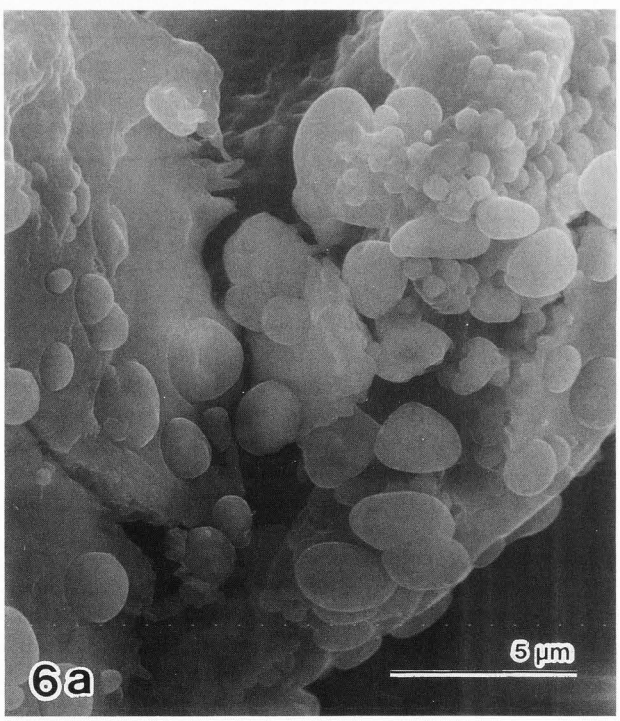

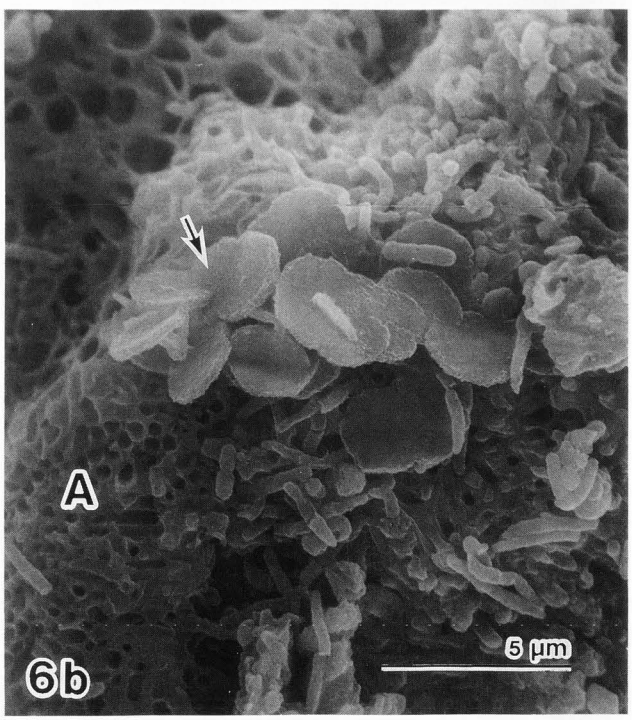

Figs. 5a, b. SEM micrographs of the type C deposits. The natural surfaces showing flake or platelet-like crystals. Samples were not treated with NaOCl.

Figs. 6a, b. SEM micrographs of crystals distinguished from the type A, B, and C deposits. **a**: oval-shaped crystals on the inner surface of calculus without NaOCl-treatment. **b**: hexagonal disk-like crystals (arrow) on the type A deposits (A) treated with NaOCl.

exceeded 1.67 (Table 2). The crystals may be HAP containing carbonate on phosphate sites [12, 35, 37]. From these Ca/P molar ratios and the thinner crystal shapes, the crystallization will be less than that in old dental calculus.

Variable crystals of the type B deposits were identified as DCPD, because the shapes and the Ca/P molar ratios of the crystals are similar to those of DCPD (Figs. 3, 4; Table 3) [3, 4, 12, 34, 37, 40-42, 46, 51, 52], and DCPD crystals are one of the major constituents of dental calculus [37, 52, 60]. These three-dimensional shapes under SEM have not been reported in dental calculus although a crystal shape on human enamel surface shown by Hoyer *et al.* [18] was about equal to our Figure 3c. The DCPD crystals were not reported in old dental calculus except in Grøns' study [17].

The crystals of the type C deposits resembled OCP rather than DCPD in their shapes and their Ca/P molar ratios (Fig. 5; Table 4) [6, 12, 29, 31, 32, 36, 37, 42, 46, 49, 52, 55]. These crystals may be OCP or the transitional forms between DCPD and OCP (DCPD-OCP) [1, 12, 37, 60].

In the other crystals, oval-shaped crystals (Fig. 6a) were similar to the type A deposits in their Ca/P molar ratio. The crystals might be Ca-deficient HAP although the oval-shaped crystals have been not reported in dental calculus.

Mg-containing hexagonal disk-like crystals (Figs. 4e, 6b) agreed with those in the old dental calculus reported in our previous study [29]. The crystals in the old calculus contained about 3 to 9 % Mg by weight and frequently coexisted with Mg-containing WHT [29], but the relationship was not elucidated and they were not identified as any crystals in the previous and also in the present study. However, it is noticeable that the hexagonal disk-like crystals were found in early as well as old dental calculus. WHT crystals, usually containing Mg, were not found in this investigation, although these crystals have been reported to be major in old calculus [12, 27, 29, 30, 32, 37, 42, 59, 60, 63].

From Schroeder's studies using TEM [57-59, 61] and the present SEM and SEM-EDX study, calculus deposits of A- and B-centers will be equal to the type A and B deposits, respectively. The type A crystals will be basically HAP as well as A-center crystals [58, 59], and both the type B and B-center crystals will be DCPD [59, 60] although the B-center crystals under the TEM were remarkably smaller than the type B crystals under the SEM. In addition, the crystals of the type C deposits may be included in B-center crystals. According to our previous studies [31, 32], long ribbon-like OCP crystals were arranged parallel and radially on the tightly packed masses of HAP in old ledge-like deposits attached to the cervical region, Therefore, the HAP masses and the ribbon-like OCP crystals will agree with the calculus deposits of A- and B-centers, respectively.

When the early dental calculus of 10 days old and up to 14 days old [57, 59, 61] are compared with the young calculus of 3 months [58, 59] and 22 to 27 days [59, 60] and also with old dental calculus [17, 20, 21, 24, 27, 29, 31, 32, 35, 42, 43, 52, 53, 55, 59, 60, 63], Ca-deficient HAP or OCP-HAP, the major crystals in the early calculus gradually mature to HAP due to an increase of pH or fluoride source [2, 6, 8, 12, 37-40, 42, 46, 48, 49, 60], and DCPD crystals which were often found in the early calculus may be gradually transformed into OCP [1, 6, 10, 34, 37], HAP [13, 40], or WHT when supplemented with Mg [9, 11, 27, 37, 42, 49, 63].

The variation of the crystal composition of calculus samples in subjects (Table 5) may be due to the difference in the pH and mineral composition of their saliva and the daily variation of the pH range [14, 19, 33, 62], since HAP and DCPD crystals are formed in different pH ranges and mineral sources [3, 12, 13, 34, 37, 40, 41, 49].

References

1. Aoba T, Ishida T, Hasegawa K, Moriwaki Y, Yamauchi T (1974). Epitaxial growth of brushite and whitlockite on the biological apatite (in Japanese). Jpn. J. Oral Biol. **16**: 252-259.

2. Aoba T, Ishida T, Yagi T, Hasegawa K, Moriwaki Y (1975). X-ray crystallographic studies on the conversion of octacalcium phosphate into hydroxyapatite (in Japanese). Jpn. J. Oral Biol. **17**: 1-7.

3. Barone JP, Nancollas GH (1978). The growth of calcium phosphates on hydroxyapatite crystals; the effect of fluoride and phosphonate. J. Dent. Res. **57**: 735-742.

4. Beevers CA (1958). The crystal structure of dicalcium phosphate dihydrate, $CaHPO_4$-$2H_2O$. Acta Cryst. **11**: 273-277.

5. Berry EE (1967). The structure and composition of some calcium deficient apatites. J. Inorg. Nucl. Chem. **29**: 317-327.

6. Brown WE, Smith JP, Lehr JR, Frazier AW (1962). Octacalcium phosphate and hydroxyapatite. Nature **196**: 1048-1055.

7. Calvo C, Gopal R (1975). The crystal structure of whitlockite from the Palermo quarry. Am. Mineral. **60**: 120-133.

8. Cheng P-T (1985). Octacalcium phosphate in vitro; implication for bone formation. Calcif. Tissue Int. **37**: 91-94.

9. Cheng P-T, Grabher JJ, LeGeros RZ (1988). Effects of magnesium on calcium phosphate formation. Magnesium **7**: 123-132.

10. Chickerur NS, Tung MS, Brown WE (1980). A mechanism for incorporation of carbonate into apatite. Calcif. Tissue Int. **32**: 55-62.

11. Daculsi G, LeGeros RZ, Jean A, Kerebel B (1987). Possible physicochemical processes in human dentin caries. J. Dent. Res. **66**: 1356-1359.

12. Driessens FCM (1982). Mineral aspect of dentistry. In: Monographs in Oral Science, Vol 10, Myers HM (ed.), Karger, Basel. pp. 12-31, 154-158.

13. Duff EG (1971). Orthophosphates II; the transformations of brushite-fluorapatite and monotite-fluorapatitein aqueous acidic KF solutions. J. Chem. Soc. Section (A), part I: 33-38.

14. Ericson T, Mäkinen KK (1986). Saliva-formation, composition and possible role. In: Textbook of Cariology, Thylstrup A, Fejerskov O (eds.), Munksgaard, Copenhagen. pp. 28-45.

15. Frondel C (1941). Whitlockite; a new calcium phosphate, $Ca_3(PO_4)$. Am. Mineral. **26**: 145-152.

16. Gonzales F, Sognnaes RF (1960). Electron microscopy of dental calculus. Science **131**: 156-158.

17. Grøn P, van Campen GJ, Lindstrom I (1967). Human dental calculus; inorganic chemical and crystallographic composition. Arch. Oral Biol. **12**: 829-837.

18. Hoyer I, Gaengler P, Bimberg R (1984). *In vivo* remineralization of human enamel and dental calculus formation. J. Dent. Res. **63**: 1136-1139.

19. Jenkins GN (1978). The Physiology and Biochemistry of the Mouth, 4th Edn. Blackwell Scientific Pub., Oxford. pp. 284-359.

20. Jensen AT, Danø M (1954). Crystallography of dental calculus and precipitation of certain calcium phosphates. J. Dent. Res. **33**: 741-750.

21. Jensen AT, Rowles SL (1967). Magnesium whitlockite; a major constituent of dental calculus. Acta Odont. Scand. **16**: 121-139.

22. Jones SJ (1972). The tooth surface in periodontal disease. Dent. Practitioner **22**: 462-473.

23. Jones SJ (1988). The root surface; an illustrated review of some scanning electron microscope studies. Scanning Microsc. **1**: 131-138.

24. Kani T, Kani M, Moriwaki Y, Doi Y (1983). Microbeam X-ray diffraction analysis of dental calculus. J. Dent. Res. **62**: 92-95.

25. Kay MI, Young RA, Posner AS (1964). Crystal structure of hydroxyapatite. Nature **204**: 1050-1052.

26. Keppler U (1965). Zum Whitlockit-Problem. Neues Jahrb. Mineral. Monatsh. **6**: 171-176.

27. Knuuttila M, Lappalainen R, Kontturi-Närhi V (1980). Effect of Zn and Mg on the formation of whitlockite in human subgingival calculus. Scand. J. Dent. Res. **88**: 513-516.

28. Kodaka T, Debari K, Yamada M (1991). Heterogeneity of crystals attached to the human enamel and cementum after calculus removal *in vitro*. Scanning Microsc. **5**: 713-721.

29. Kodaka T, Debari K, Higashi S (1988). Magnesium containing crystals in human dental calculus. J. Electron Microsc. **37**: 73-80.

30. Kodaka T, Hirayama A, Miake K, Higashi S (1989). Bacillus-shaped deposits composed of hexahedrally based crystals in human dental calculus. Scanning Microsc. **3**: 843-854.

31. Kodaka T, Ishida I (1984). Observations of plate-like crystals in human dental calculus. Bull. Tokyo Dent. Coll. **25**: 131-138.

32. Kodaka T, Miake K (1991). Inorganic components and the fine structures of marginal and deep subgingival calculus. Bull. Tokyo Dent. Coll. **32**: 99-110.

33. Lagerlöf F (1983). Effects of flow rate and pH on calcium phosphate saturation in human parotid saliva. Caries Res. **17**: 403-411.

34. LeGeros RZ (1972). Brushite crystals grown by diffusion in silica gel and in solution. J. Crystal Growth **13/14**: 476-480.

35. LeGeros RZ (1974). Variation in the crystalline components of human dental calculus I; crystallographic and spectroscopic methods of analysis. J. Dent. Res. **54**: 45-50.

36. LeGeros RZ (1985). Preparation of octacalcium phosphate (OCP); a direct fast method. Calcif. Tissue Int. **37**: 194-197.

37. LeGeros RZ (1991). Calcium phosphates in oral biology and medicine. In: Monographs in Oral Science, Vol 15, Myers HM (ed.), Karger, Basel, pp. 1-201.

38. LeGeros RZ, Daculsi G, Orly I, Torres W (1989). Solution-mediated transformation of octacalcium phosphate (OCP) to apatite. Scanning Microsc. **3**: 129-138.

39. LeGeros RZ, Kijkowska R, LeGeros JP (1984). Formation and transformation of octacalcium phosphate, OCP; a preliminary report. Scanning Electron Microsc. **1984**;IV: 1771-1777.

40. LeGeros RZ, Lee D, Quirolgico G, Shirra WP, Reich L (1983). *In vitro* formation of dicalcium phosphate dihydrate, $CaHPO_4$-$2H_2O$ (DCPD). Scanning Electron Microsc. **1983**;I: 407-418.

41. LeGeros RZ, LeGeros JP (1972). Brushite crystals grown by diffusion. J. Crystal Growth **13**: 476-480.

42. LeGeros RZ, Orly I, LeGeros JP, Gomez C, Kazimiroff J, Tarpley T, Kerebel B (1988). Scanning electron microscopy and electron probe microanalysis of the crystalline components of human and animal dental calculi. Scanning Microsc. **2**: 345-356.

43. Lustmann J, Lewin-Epstein J, Shteyer A (1976). Scanning electron microscopy of dental calculus. Calcif. Tissue Res. **21**: 47-55.

44. Mandel ID, Levy BM, Wasserman BH (1957). Histochemistry of dental calculus formation. J. Periodontol. **28**: 132-137.

45. Marthaler TM, Schroeder HE, Möhlemann HR (1961). A method for the quantitative assessment of plaque and calculus formation. Helv. Odont. Acta **5**: 39-42.

46. Moriwaki Y, Doi Y, Kani Y, Aoba T, Takahashi J, Okazaki M (1983). Synthesis of enamel-like apatite at physiological temperature and pH using ion-selective membranes. In: Mechanisms of Tooth Enamel Formation, Suga S (ed.), Quintessence Pub., Tokyo. pp. 239-256.

47. Mühlemann HR, Schneider UK (1959). Early calculus formation. Helv. Odont. Acta **3**: 22-26.

48. Nelson DGA, McLean JD (1984). High-resolution electron microscopy of octacalcium phosphate and its hydrolysis products. Calcif. Tissue Int. **36**: 219-232.

49. Newesely H (1965). Über die Existenzbedingungen von Oktacalciumphosphat, Whitlockit und Carbonatapatit. Dtsch. Zahnäerztl. Z. **20**: 753-766.

50. Posner AS (1969). Crystal chemistry of bone mineral. Physiol. Rev. **49**: 760-792.

51. Rodgers AL, Spector M (1986). Pancreatic calculi containing brushite; ultrastructure and pathogenesis. Calcif. Tissue Int. **39**: 342-347.

52. Rowles SL (1964). Biophysical studies on dental calculus in relation to periodontal disease. Dent. Practit. **5**: 2-7.

53. Ruzicka F (1984). Structure of sub- and supragingival dental calculus in human periodontics; an electron microscopic study. J. Periodontal Res. **19**: 317-327.

54. Santos M, Gonzalez-Diaz PF (1980). Ultrastructural study of apatites in human urinary calculi. Calcif. Tissue Int. **31**: 93-108.

55. Saxton CA (1968). Identification of octacalcium phosphate in human dental calculus by electron diffraction. Arch. Oral Biol. **13**: 243-246.

56. Schroeder HE (1963). Inorganic content and histology of early dental calculus in man. Helv. Odont. Acta **7**: 17-30.

57. Schroeder HE (1964). Two different types of mineralization in early dental calculus. Helv. Odont. Acta **8**: 117-127.

58. Schroeder HE (1965). Crystal morphology and gross structures of mineralizing plaque and calculus. Helv. Odont. Acta **9**: 73-86.

59. Schroeder HE (1969). Formation and Inhibition of Dental Calculus. Hans Huber, Berne, pp. 94-122.

60. Schroeder HE, Bambauer HU (1966). Stages of calcium phosphate crystallization during calculus formation. Arch. Oral Biol. **11**: 1-14.

61. Schroeder HE, Lenz H, Mühlemann HR (1963). Mineralization centers in early dental calculus formation by light and electron microscopy. Helv. Odont. Acta **7**: 67-75.

62. Suddick RP, Hyde R, Feller RP (1980). Salivary water and electrolytes and oral health. In: The Biologic Basis of Dental Caries, Menaker L (ed.), Harper & Row Pub., Hagerstown. pp. 132-147.

63. Sundberg M, Friskopp J (1985). Crystallography of subgingival human dental calculus. Scand. J. Dent. Res. **93**: 30-38.

64. Turesky S, Renstrup G, Glickman I (1961). Histologic and histochemical observations regarding early calculus formation in children and adults. J. Periodontol. **32**: 7-14.

Discussion with Reviewers

R.Z. LeGeros: Your study is well done and provide very interesting results important to our understanding of calculus formation and composition. Was there a significant difference in the composition of calculus that could be related to the age of the subjects?

Authors: In this study, we could not reveal this due to the small number of samples. Turesky *et al.* [64] reported that the calculus formation on cellulose strips occurred less rapidly in children than in adults, but presented the same histologic and histochemical features. According to our previous SEM study using exfoliated deciduous teeth with attached dental calculus [65], the calculus contained HAP-, OCP-, and WHT-like crystals, although these amounts might be smaller than those in adults [29-31]. These reports suggest that there are no difference in the composition between children and adults.

R.Z. LeGeros: What values for %Ca and %P were obtained for the F-Apatite used as standard for the analyses?

Authors: So far, for the quantitative analysis of Ca and P, we have used the standard sample of native fluorapatite and applied the ZAF corrections [28-32].

Reviewer II: It is highly questionable whether the manuscript presents sufficient data in order to conclude the frequency of crystals having various shapes and morphologies.

Authors: The aim of this study was to illustrate the three dimensional crystal shapes of early calculus using SEM and SEM-EDX. We have not analyzed the statistics of these crystals due to a small number of samples (eight subject). We use "frequency" in the paper to mean tendency.

G. Daculsi: Have you determined the amount of sulphur and magnesium and did you observe a relation with the three types of crystals (A,B,C)?

Authors: No we did not. Under the SEM-EDX analysis, a small amount of sulphur was detected only in dental plaque (PQ in Figs. 1, 3; MO in Fig. 2). Magnesium was detected only in hexagonal disk-like crystals (Fig. 6b), but the Ca, P, and Mg contents could not be quantitatively analyzed due to the very small mass of the crystals [29].

Reviewer III: SEM-EDX data from samples treated with NaOCl are lacking. The material used for EDX analysis is heavily contaminated with such organic material as bacteria, salivary secretion, etc. How can it give the true analysis of the calculus?

Authors: When the SEM-EDX data on dental hard tissues treated with and without NaOCl are compared [66], the Ca and P contents in the NaOCl-treated cementum showed 34.00 $\pm$ 0.23 and 15.74 $\pm$ 0.10% by weight, respectively (Ca/P molar ratio was 1.68 $\pm$ 0.01), while

those in the untreated cementum obtained from the same tooth showed 22.80 ± 0.42 and 10.89 ± 0.16% (Ca/P molar ratio was 1.62 ± 0.03). Thus, there were significant differences between the samples. The Ca content in the NaOCl-treated cementum was nearly equal to the Ca content of the untreated (36.08 ± 0.27%) and NaOCl-treated enamel (35.75 ± 0.21%) obtained from the same tooth. A NaOCl solution may more or less dissolve organic matters in mineralized tissues and the regions which have included organic matter will be filled with water, ethanol, and air following sample procedure. Under SEM-EDX analysis, the sample must be in a high vacuum, thereby the air spaces will be in vacuum. From the above-mentioned EDX data, the empty spaces are not accounted as the sample regions under the EDX analysis. When cementum and dental calculus containing a relatively large amount of organic matter are treated with NaOCl, they must be embedded in resin under EDX analysis. Such an EDX analysis will be the data of crystals composed of NaOCl-insoluble minerals. In this EDX analysis, however, we have not undertaken such methods; therefore, non-crystallized Ca and P besides Ca and P in crystals may have been detected.

Additional References

65. Higashi S, Kawahara T, Nakagawa T, Nakajima F, Hanai M, Kodaka T, Suzuki Y, Sasa R (1981). Histological study on dental calculi attached to human deciduous teeth (in Japanese). Jpn. J. Ped. Dent. **19**: 448-460.

66. Kodaka T (1984). SEM images and XMA analysis of hard tissue treated with NaOCl (in Japanese). Acta Anat. Nippon. **59**: 486.